

Nonlinear corrections to the cosmological matter power spectrum and scale-dependent galaxy bias: implications for parameter estimation

Jan Hamann

LAPTH (Laboratoire d'Annecy-le-Vieux de Physique Théorique, CNRS UMR5108 & Université de Savoie), BP 110, F-74941 Annecy-le-Vieux Cedex, France

Steen Hannestad

Department of Physics and Astronomy, University of Aarhus
Ny Munkegade, DK-8000 Aarhus C, Denmark

Alessandro Melchiorri

Physics Department and sezione INFN, University of Rome "La Sapienza"
Ple Aldo Moro 2, I-00185 Rome, Italy

Yvonne Y. Y. Wong

Max-Planck-Institut für Physik (Werner-Heisenberg-Institut)
Föhringer Ring 6, D-80805 München, Germany

E-mail: hamann@lapp.in2p3.fr, sth@phys.au.dk,
alessandro.melchiorri@roma1.infn.it, ywong@mppmu.mpg.de

Abstract. We explore and compare the performances of two nonlinear correction and scale-dependent biasing models for the extraction of cosmological information from galaxy power spectrum data, especially in the context of beyond- Λ CDM cosmologies. The first model is the well known Q model, first applied in the analysis of 2dFGRS data. The second, the P model, is inspired by the halo model, in which nonlinear evolution and scale-dependent biasing are encapsulated in a single non-Poisson shot noise term. We find that while both models perform equally well in providing adequate correction for a range of galaxy clustering data in standard Λ CDM cosmology and in extensions with massive neutrinos, the Q model can give unphysical results in cosmologies containing a subdominant free-streaming dark matter whose temperature depends on the particle mass, e.g., relic thermal axions, unless a suitable prior is imposed on the correction parameter. This last case also exposes the danger of analytic marginalisation, a technique sometimes used in the marginalisation of nuisance parameters. In contrast, the P model suffers no undesirable effects, and is the recommended nonlinear correction model also because of its physical transparency.

1. Introduction

The past decade saw an explosion of precision cosmological measurements. Foremost amongst these is the observation of temperature and polarisation fluctuations in the cosmic microwave background (CMB) by a range of experiments [1–6]. The distribution of large-scale structures (LSS) has also been mapped to unprecedented breadths and depths by galaxy redshift surveys such as the Two-Degree Field Galaxy Redshift Survey (2dFGRS) [7] and the Sloan Digital Sky Survey (SDSS) [8, 9]. Together with observations of distant type Ia supernovae [10, 11], these measurements have fostered the emergence of a benchmark framework—the adiabatic, nearly scale-invariant, “vanilla” Λ CDM model—based on which one can test for evidence of new physics.

Clustering statistics of galaxies as probed by surveys like 2dF and SDSS are particularly well suited for the exploration of physics that introduce new effects on length scales $\mathcal{O}(10) \rightarrow \mathcal{O}(100) h^{-1}$ Mpc. A classic example is the possibility to detect a subdominant component of free-streaming hot dark matter (HDM) [12], notably massive neutrinos [13, 14] and variants such as thermal axions [15–19], light gravitinos [20], *et cetera*. The sensitivity of these surveys at small length scales also lends a greater lever arm to the search for features in the primordial density perturbation power spectrum, possible remnants of inflationary physics [21, 22]. Last but not least, since the power spectrum of large-scale structures probes uniquely the parameter combination $\Omega_m h$, it helps to lift the degeneracy between—and hence tighten the constraints on—the physical matter density $\Omega_m h^2$ and the Hubble parameter h from CMB observations alone.

Usage of data from galaxy clustering surveys is based on the premise that one can reliably predict the distribution of galaxies, at least on a statistical basis, from theory. This is complicated by a number of factors. First, galaxies are necessarily collapsed objects, i.e., they have undergone a phase of nonlinear evolution. Using them as tracers of the underlying matter field implicitly assumes we know how to relate the two distributions to one another. A reasonable assumption is that on sufficiently large scales the power spectra of galaxies and of the matter field are identical up to a constant normalisation, or bias, factor. But this bias relation is expected to become scale-dependent when the dimensionless power spectrum of the galaxies $\Delta_{\text{gal}} \equiv k^3 P_{\text{gal}}/2\pi^2$ exceeds unity [23, 24]. Indeed, the apparent tension between the 2dF and the SDSS galaxy power spectra is now believed to have originated from a more strongly scale-dependent bias factor for the red galaxies dominating the SDSS galaxy catalogue [25, 26]. On the theoretical front, a good deal of recent effort has also been devoted to understanding the origin of scale-dependent biasing (e.g., [27, 28]).

Second, galaxy positions are inferred from their redshifts. However, the peculiar motions of the galaxies, particularly when amplified by virialisation, induce additional Doppler shifts that can potentially obscure the inference. This is known as redshift space distortion, and on small length scales requires corrections beyond linear perturbation theory. Third, the clustering of the underlying dark matter field itself becomes nonlinear on scales $k \gtrsim 0.2 h \text{ Mpc}^{-1}$. Thus, how reliably one can extract cosmological information

from galaxy clustering statistics depends crucially on how well one can model these three nonlinear effects.

While all three effects can in principle be modelled by numerical simulations, these simulations, and indeed our understanding of galaxy formation, are not yet at a stage where one can reliably predict the power spectrum of galaxies as a function of galaxy type and redshift given some underlying cosmological model. In the meantime, nonlinear evolution and scale-dependent biasing must be modelled empirically as a systematic effect and the associated nuisance parameters marginalised when extracting cosmological information from galaxy clustering surveys, especially in beyond- Λ CDM cosmologies.

In this connection, Cole *et al.* [7] recently proposed a correction formula which maps directly between the matter power spectrum calculated from linear perturbation theory $P_{\text{lin}}(k)$ and the power spectrum expected for the galaxies $P_{\text{gal}}(k)$,

$$P_{\text{gal}}(k) = b^2 \frac{1 + Q_{\text{nl}} k^2}{1 + A_{\text{nl}} k} P_{\text{lin}}(k). \quad (1.1)$$

The formula is partially calibrated against Λ CDM-based semi-analytic galaxy formation simulations ($A_{\text{nl}} = 1.4$ for redshift space, and 1.7 for real space), and contains two free parameters (b and Q_{nl}) to be fixed by observational data. Equation (1.1) has been applied to the galaxy power spectra of 2dF [7] and the SDSS luminous red galaxy (LRG) sample [8] to test standard vanilla cosmology. However, there is *a priori* no guarantee that its usefulness extends also to cosmologies beyond Λ CDM. Indeed, as we shall show below, equation (1.1) can be highly pathological when applied to certain classes of cosmological models containing a subdominant component of free-streaming dark matter.

In comparison, a conceptually more appealing framework in which to discuss nonlinear corrections is the halo model [29–32]. Building on the assumptions of (i) hierarchical clustering, and (ii) that galaxies form only inside dark matter halos, halo model-based nonlinear corrections can in principle be made applicable to all hierarchical CDM cosmologies. The minimal model proposed in references [33–35], for example,

$$P_{\text{gal}}(k) = b^2 P_{\text{lin}}(k) + P_{\text{shot}}, \quad (1.2)$$

where b and P_{shot} are free parameters, does not demand vanilla Λ CDM as the sole input cosmology.

In the present work, we explore and compare the performance of these nonlinear correction models in some detail. We confront them with various observed galaxy power spectra, especially in the context of beyond- Λ CDM cosmologies. We discuss parameter degeneracies and the role of priors on the nuisance parameters.

The paper is organised as follows. We describe first in section 2 the galaxy clustering data sets used in the analysis. Section 3 contains a more detailed discussion of the two nonlinear models we wish to explore. In sections 4, 5 and 6 we test the nonlinear models against data for standard vanilla cosmology, vanilla with massive neutrinos, and vanilla with thermal axions respectively. We conclude in section 7.

2. Data sets

We use the publicly available galaxy power spectra from the following galaxy catalogues.

2dF This data set comes from the final data release of the Two-Degree Field Galaxy Redshift Survey [7]. We use up to 36 data bands, corresponding to redshift space power spectrum data for wavenumbers $0.02 \lesssim k/h \text{ Mpc}^{-1} \lesssim 0.18$.

SDSS-2 main Real space power spectrum of the main galaxy sample from the Sloan Digital Sky Survey data release 2 [36]. We use up to 19 data bands, i.e., $0.016 \lesssim k/h \text{ Mpc}^{-1} \lesssim 0.2$.

SDSS-4 LRG Real space power spectrum of the luminous red galaxies from the Sloan Digital Sky Survey data release 4 [8]. The 20 data bands correspond to wavenumbers $0.012 \lesssim k/h \text{ Mpc}^{-1} \lesssim 0.2$.

WMAP-3 We also use at times CMB data from the Wilkinson Microwave Anisotropy Probe experiment after three years of observations [37–39], mainly for the construction of priors on certain cosmological parameters. This calculation is performed using version 2 of the likelihood package provided by the WMAP team on the LAMBDA web page [40].

3. Two nonlinear models

3.1. The Q model

We refer to the correction formula (1.1) as the Q model. For Λ CDM cosmologies, galaxy formation simulations suggest that the parameter A_{nl} can be held fixed at $A_{\text{nl}} = 1.4$ in redshift space and at $A_{\text{nl}} = 1.7$ in real space [7]. The parameter Q_{nl} , however, exhibits a strong dependence on the galaxy type. Fitting the Q model to the 2dF galaxy power spectrum at $0.02 \lesssim k/h \text{ Mpc}^{-1} \lesssim 0.3$, Cole *et al.* found $Q_{\text{nl}} = 4.6 \pm 1.5$ for vanilla cosmology [7]. Tegmark *et al.* [8] applied the same model to SDSS-4 LRG, for which $Q_{\text{nl}} = 30 \pm 4$ provides a good fit.†

Note that the case of $Q_{\text{nl}} = 0$ is not equivalent to no nonlinear correction, since a nonzero A_{nl} parameter also modulates the power spectrum in a scale-dependent way. For $Q_{\text{nl}} \lesssim 7$, the Q model suppresses the power spectrum at $k \lesssim 0.2 h \text{ Mpc}^{-1}$. However, for Q_{nl} values as large as 30 such as required by the SDSS-4 LRG, the main role of the Q model is to add power at $k \gtrsim 0.07 h \text{ Mpc}^{-1}$.

† Tegmark *et al.* [8] used $A_{\text{nl}} = 1.4$, although strictly speaking $A_{\text{nl}} = 1.7$ is the more appropriate value for the real space power spectrum of SDSS-4 LRG. However, at the present level of precision, our tests show that adopting the correct $A_{\text{nl}} = 1.7$ only causes a statistically insignificant upward shift in the best-fit Q_{nl} ($\Delta Q_{\text{nl}} \sim 2$), while the estimates of other cosmological parameters remain unaffected. Henceforth we shall use exclusively $A_{\text{nl}} = 1.4$ for both real and redshift space power spectra.

3.2. The P model

The functional form of the Q model (1.1) was recently criticised in reference [28] for its incorrect dependence on k . Specifically, it lacks a constant term to account for the presence of non-Poisson shot noise, a generic consequence of the assumption that galaxies form exclusively in halos. Indeed, from the halo model [29–32], one should expect a correction formula with the skeletal form,

$$P_{\text{gal}}(k) = P_{2\text{h}}(k) + P_{1\text{h}}(k). \quad (3.1)$$

Here, the two-halo term, $P_{2\text{h}}(k) = b^2(k)P_{\text{lin}}(k)$, arises from correlations between galaxies in two different halos, and approximates the familiar linear bias relation on large scales,

$$P_{2\text{h}}(k) \approx b^2 P_{\text{lin}}(k). \quad (3.2)$$

The one-halo term

$$P_{1\text{h}}(k) \approx \text{const.} \equiv P_{\text{shot}} \quad (3.3)$$

accounts for correlations within the same halo and is approximately independent of the exact spatial distribution of the galaxies within a halo provided k is not too large. Combining equations (3.2) and (3.3) we recover the minimal model (1.2).

The role of the shot noise term P_{shot} is to add power at small length scales, so that the ratio $P_{\text{gal}}(k)/P_{\text{lin}}(k)$ is effectively scale-dependent at large k values. This is in contrast with the Q model (1.1), which for some values of the nonlinear parameter Q_{nl} suppresses the power spectrum on the observable scales. Interestingly, taken at face value, the P model also predicts a significant k -dependence for $P_{\text{gal}}(k)/P_{\text{lin}}(k)$ as $k \rightarrow 0$ when P_{shot} once again rises above $b^2 P_{\text{lin}}(k) \sim k$ [29]. It should be noted however that this small- k behaviour is not present for dark matter clustering, since momentum conservation demands that the dark matter power spectrum falls off faster than $P(k) \propto k^4$ as $k \rightarrow 0$ [41], a behaviour also observed in numerical simulations [42, 43]. On the other hand, a non-vanishing shot noise on large scales is in principle not forbidden for galaxy clustering, since tracers need not conserve momentum. Whether or not this is so remains to be understood.

In the present work we take the view that since galaxy clustering has not been observed on scales where the shot noise behaviour may become problematic ($k \ll 0.01 h \text{ Mpc}^{-1}$), equation (1.2) constitutes a sufficient phenomenological model to describe the galaxy power spectrum at $k \gtrsim 0.01 h \text{ Mpc}^{-1}$.

Additional modifications to the basic P model (1.2) to account for the damping of baryon acoustic oscillations and other nonlinear mode coupling effects have been discussed in the literature [28, 43–45]. These generally lead to nonlinear models of the form

$$P_{\text{gal}}(k) = b^2 A(k) P_{\text{lin}}(k) + P_{\text{shot}}, \quad (3.4)$$

where $A(k)$ is some function of k that depends also on the galaxy type. It is also possible to extend the halo model to include redshift space distortion [35, 45, 46]. We ignore these additional corrections in the present analysis in order to keep the number of extra

fit parameters to a minimum. However, we emphasise that the effects encapsulated by $A(k)$ will become increasingly important as more precise data from future galaxy redshift surveys become available.

4. Test 1: vanilla

4.1. Set-up

To compare the performance of the two nonlinear models, we test them against galaxy clustering data in three minimal parameter spaces:

- (i) $\Omega_m h, \Omega_b h^2, h, n_s, \ln(10^{10} \mathcal{A})$,
- (ii) $\Omega_m h, \Omega_b h^2, h, n_s, \ln(10^{10} \mathcal{A}), P_{\text{shot}}$, and
- (iii) $\Omega_m h, \Omega_b h^2, h, n_s, \ln(10^{10} \mathcal{A}), Q_{\text{nl}}$.

We take the geometry of the universe to be flat, and the initial conditions adiabatic. The parameter $\mathcal{A} \equiv b^2 A_s$ accounts for the normalisation of the galaxy power spectrum, and incorporates both the amplitude of the primordial scalar perturbations A_s and the constant galaxy bias factor b . We do not use any nonlinear correction for parameter space (i), i.e., $P_{\text{gal}}(k) = b^2 P_{\text{lin}}(k)$. For parameter spaces (ii) and (iii), we use the P model (1.2) and the Q model (1.1) respectively.

Note the definition of the matter density parameter $\Omega_m h$. We choose this parameterisation because the turning point of the matter power spectrum is sensitive to the comoving Hubble radius at matter–radiation equality, which, for fixed values of h , depends on $\Omega_m h$, not the physical matter density $\Omega_m h^2$. For fixed values of n_s and h , $\Omega_m h$ alone determines the broad shape of the matter power spectrum within the Λ CDM framework.

We use standard Bayesian inference techniques and the Markov Chain Monte Carlo package COSMOMC [47, 48] to explore the posterior hypersurfaces as functions of the model parameters and the galaxy clustering data sets of section 2. Here, we note that within the vanilla framework, the physical baryon density $\Omega_b h^2$, the Hubble parameter h , and the scalar spectral index n_s can be individually well constrained by CMB observations. This information is encapsulated in a set of “WMAP-3 priors” in table 1, which we apply when varying these three parameters. This approach differs slightly from the more common practice of fixing the parameter values $h = 0.72$ and $n_s = 1$ adopted in, e.g., references [7, 26]. Reference [8] further fixes $\Omega_b h^2 = 0.0223$. Our approach has the advantage that it properly takes into account the uncertainties on these parameters and thus avoids two inherent dangers of fixed parameter analyses: biased parameter estimates and underestimated errors. Additionally, it permits a consistent comparison of our $\Omega_m h$ constraints not only between different galaxy clustering data sets, but also with those obtained from CMB observations alone.

Broad, top-hat priors are imposed on the remaining parameters (table 1). For the parameter Q_{nl} , we choose the range 0–50 for all three data sets. In the absence of additional information from, e.g., galaxy formation simulations, the upper limit

Table 1. Priors used in our vanilla and vanilla+massive neutrinos analyses. *Top:* WMAP priors based on the three-year data release. These are approximated as perfect Gaussians, and we give here their respective mean and standard deviation. *Bottom:* Top-hat priors for the remaining parameters.

Parameter	vanilla	vanilla+neutrinos
WMAP-3 priors		
$\Omega_b h^2$	0.02229 ± 0.00073	0.02158 ± 0.00082
h	0.732 ± 0.032	0.651 ± 0.054
n_s	0.958 ± 0.016	0.941 ± 0.022
Top-hat priors		
$\Omega_m h$	0.05–0.72	
$\ln(10^{10} \mathcal{A})$	1–5	
P_{shot}	0– $\min(P_{\text{obs}})$	
Q_{nl}	0–50	

of this prior is somewhat arbitrary. We will discuss this point in more detail in section 6. For the P_{shot} prior, the upper limit $\min(P_{\text{obs}})$ denotes the minimum clustering power measured by a survey. In other words, the linear matter power spectrum $P_{\text{lin}}(k)$ must not be negative anywhere. For 2dF, SDSS-2 main, and SDSS-4 LRG, $\min(P_{\text{obs}}) = \{4000, 1200, 9300\}$, respectively.

4.2. The internal test: do the individual data sets call for nonlinear correction?

Figures 1 to 3 show the 1D marginal constraints on the parameters $\{\Omega_m h, P_{\text{shot}}, Q_{\text{nl}}\}$ and the corresponding minimum χ^2 and numbers of degrees of freedom (d.o.f.) as functions of the maximum wavenumber k_{max} included in the analysis. The number of d.o.f. is defined here as the number of data points plus the number of priors, minus the number of fit parameters; its actual value might be slightly lower, because the power spectrum data points are not completely uncorrelated owing to overlapping window functions.

For $\Omega_m h$, the green/shaded regions correspond to the 1D marginal 68% minimum credible intervals (MCI), while the 1D modes are indicated by black/dotted lines. On the other hand, the marginalised posterior distributions in P_{shot} and Q_{nl} are often extremely flat, especially at small values of k_{max} . While it is technically possible to construct credible intervals in these cases, quoting such an interval would distract from the fact that the parameters are essentially unconstrained. Therefore, instead of Bayesian intervals, we give in figures 1 to 3 for P_{shot} and Q_{nl} the parameter regions satisfying

$$-2(\ln \mathcal{P} - \ln \mathcal{P}_{\text{max}}) < 1, \quad (4.1)$$

where \mathcal{P} is the 1D marginal posterior and \mathcal{P}_{max} denotes its value at the 1D mode. We loosely label this the “ 1σ ” interval. For large k_{max} values, especially $k_{\text{max}} \sim 0.2 h \text{ Mpc}^{-1}$, where the posterior distributions are approximately Gaussian, this 1σ interval is identical

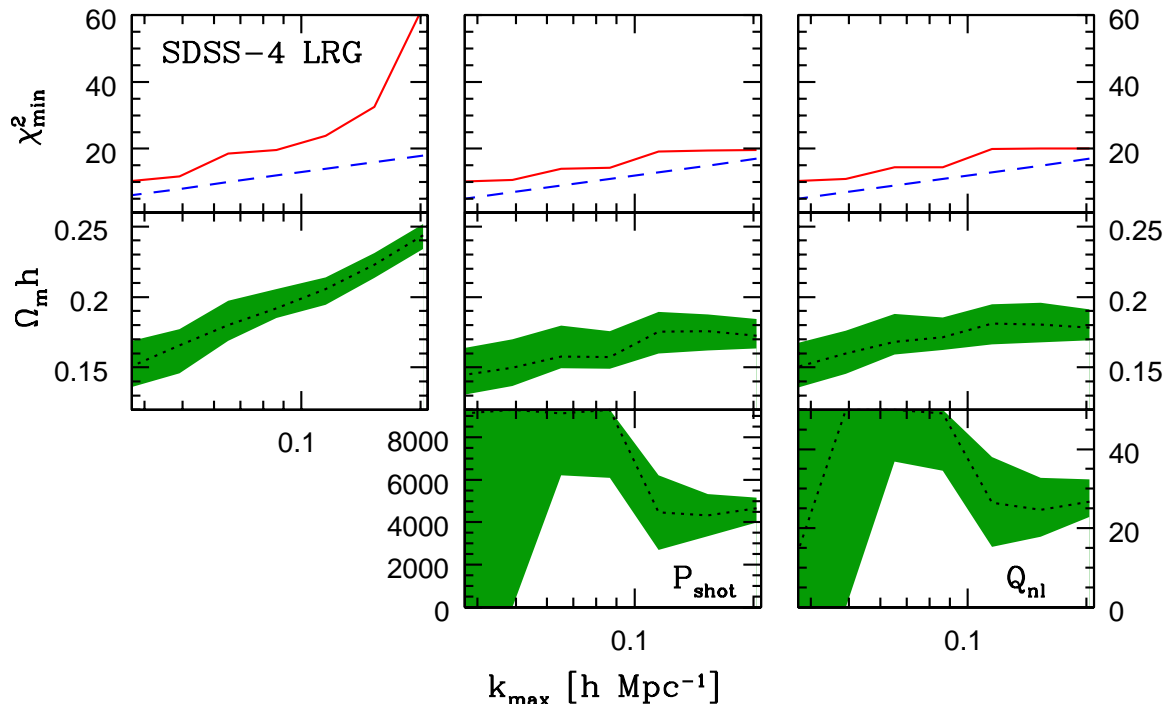


Figure 1. 1D marginal 68% MCIs for $\Omega_m h$ and 1σ intervals (see main text for definitions) for the nonlinear parameters P_{shot} and Q_{nl} as functions of k_{max} using the SDSS-4 LRG power spectrum (green/shaded regions). *Left:* No nonlinear correction. *Centre:* Correction with the P model. *Right:* Correction with the Q model. In each case the black dotted line indicates the 1D mode. The top plot in each column shows the minimum χ^2 (red/solid) and the number of degrees of freedom in the fit (blue/dash).

to the 68% MCIs. See reference [49] for more detailed discussions of the various statistical quantities.

Changes in the $\Omega_m h$ estimates The effects of nonlinear correction are most evident when we include data beyond $k_{\text{max}} \sim 0.1 h \text{ Mpc}^{-1}$. Here, nonlinear correction generally shifts the $\Omega_m h$ estimates to lower values relative to the case with no correction, irrespective of the nonlinear model used. For SDSS-4 LRG, this shift is very dramatic: at $k_{\text{max}} \sim 0.2 h \text{ Mpc}^{-1}$ the 68% MCI moves down by an amount comparable to six or seven times its half-width (figure 1). In contrast, the shifts induced for 2dF and SDSS-2 main by either nonlinear model are mild: at $k_{\text{max}} \sim 0.2 h \text{ Mpc}^{-1}$ a small overlap between the 68% MCIs before and after correction can still be seen in figures 2 and 3.

The χ^2 test The need for nonlinear correction in the case of SDSS-4 LRG is corroborated by a comparison of the minimum χ^2 values. Between correction and no correction, figure 1 shows that at $k_{\text{max}} \sim 0.2 h \text{ Mpc}^{-1}$, χ_{min}^2 changes from ~ 60 for 18 d.o.f. to ~ 20 for 17 d.o.f., again irrespective of the nonlinear model used. On the other hand, similar comparisons for 2dF and for SDSS-2 main in figures 2 and 3 do not

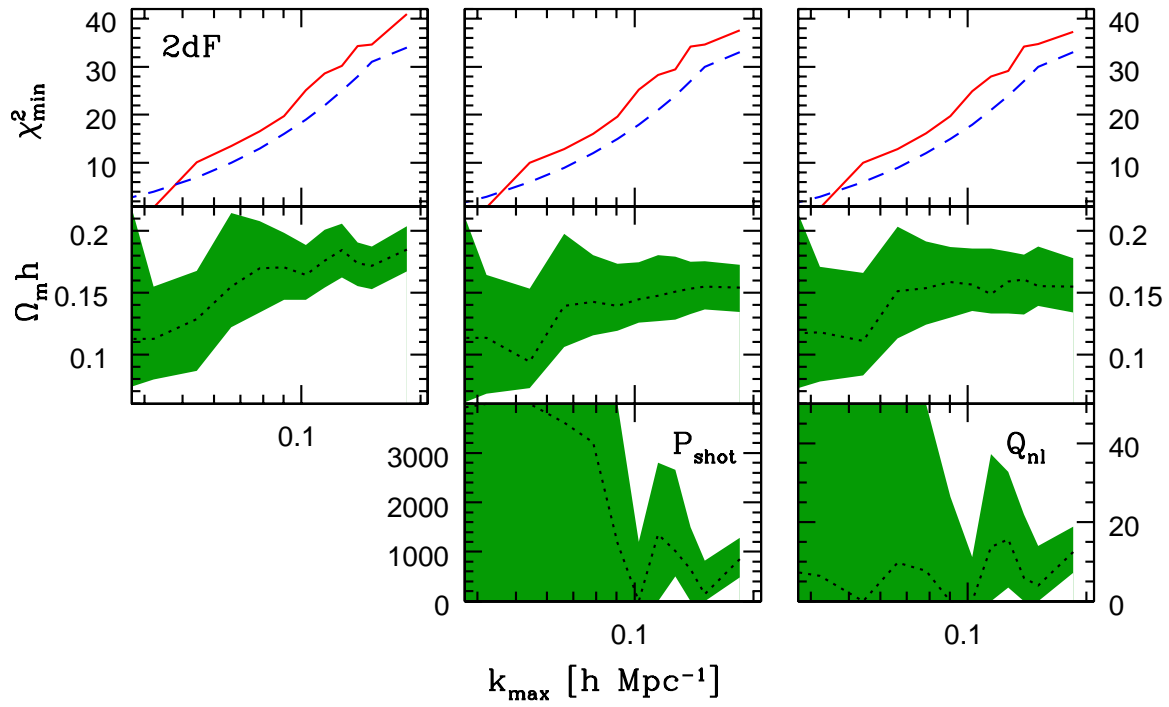


Figure 2. Same as figure 1, but for 2dF.

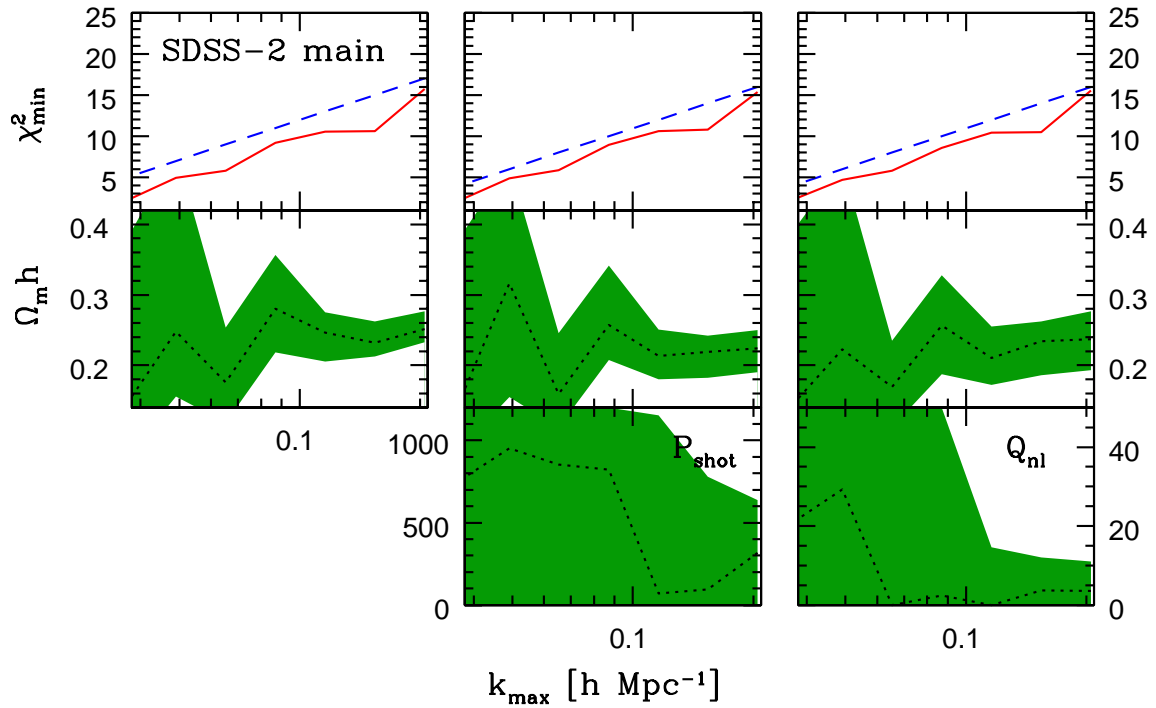


Figure 3. Same as figure 1, but for SDSS-2 main.

indicate any urgent need for an extra correction parameter: for 2dF, $\Delta\chi_{\min}^2 \sim 4$; for SDSS-2 main, $\Delta\chi_{\min}^2$ is virtually negligible.

Internal consistency We consider a data set internally consistent if the $\Omega_m h$ credible intervals agree for all choices of k_{\max} . For SDSS-4 LRG, figure 1 clearly demonstrates that nonlinear correction is necessary in order to achieve some semblance of internal consistency. A small discrepancy remains after correction: at $k_{\max} \sim 0.03$ and $0.2 h \text{ Mpc}^{-1}$ the 68% MCIs do not quite touch each other. However, this discrepancy is not statistically significant. We bring up this point here nonetheless as a cautionary note against over-interpretation of credible intervals.

Nonlinear correction also helps to improve consistency in the $\Omega_m h$ estimates from 2dF in figure 2. As for SDSS-2 main, the large uncertainties in $\Omega_m h$ in figure 3 means that internal consistency is not an issue, with or without nonlinear correction.

How much correction? Focussing on the cases with nonlinear correction, we see in figures 1 to 3 that while SDSS-4 LRG clearly prefers a nonzero correction parameter—be it P_{shot} or Q_{nl} —at $k_{\max} \gtrsim 0.1 h \text{ Mpc}^{-1}$, the 2dF and the SDSS-2 main data sets do not exhibit the same strong preference. For SDSS-2 main and most choices of k_{\max} for 2dF, the 1σ regions include $P_{\text{shot}} = 0$ and $Q_{\text{nl}} = 0$ (although, as mentioned before, the case of $Q_{\text{nl}} = 0$ is not equivalent to no nonlinear correction). At $k_{\max} \lesssim 0.1 h \text{ Mpc}^{-1}$, the parameters P_{shot} and Q_{nl} cannot be constrained by data.

In terms of the P model, roughly half of the small scale ($k \gtrsim 0.1 h \text{ Mpc}^{-1}$) power in SDSS-4 LRG can be attributed to the shot noise term. For 2dF and SDSS-2 main, the shot noise contribution is about a quarter according to the 1D mode.

Which nonlinear model? Perhaps the most striking feature about the two nonlinear models considered here is that their corrective effects appear to be identical. This is particularly apparent in figures 1 and 2 at $k_{\max} \gtrsim 0.1 h \text{ Mpc}^{-1}$, where the preferred values of the correction parameters P_{shot} and Q_{nl} exhibit virtually the same dependence on k_{\max} . At $k_{\max} \sim 0.2 h \text{ Mpc}^{-1}$ the $\Omega_m h$ estimates also show little if any dependence on the priors imposed on the nonlinear correction parameters. Thus as far as vanilla cosmology is concerned, there is no preference for either nonlinear model from a phenomenological standpoint, although the transparency of the P model still makes it the more attractive one of the two.

4.3. The external test: are all data sets consistent with each other?

Figure 4 shows how the constraints on $\Omega_m h$ obtained from different galaxy clustering data sets and with different nonlinear correction methods compare with each other. For good comparison we indicate in the figure also the corresponding estimate from WMAP-3. Similar information is available in table 2, in which we give the 1D marginal 68% and 95% MCIs at $k_{\max} \sim 0.2 h \text{ Mpc}^{-1}$ ($k_{\max} \sim 0.18 h \text{ Mpc}^{-1}$ for 2dF).

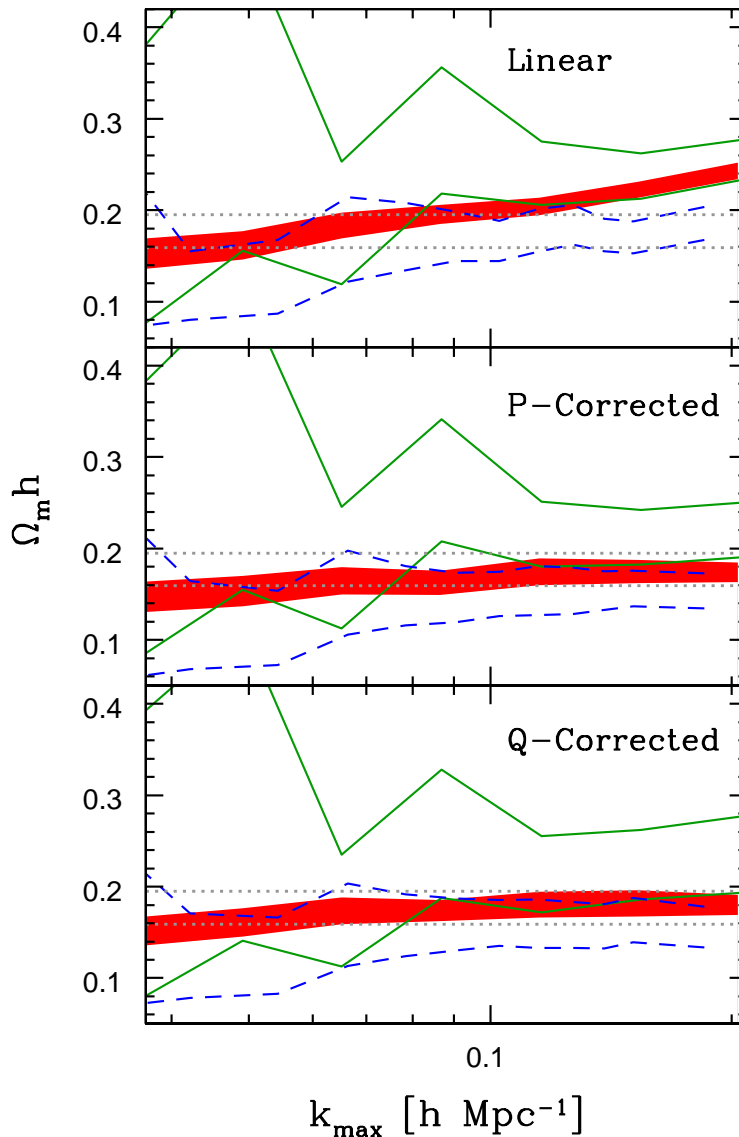


Figure 4. 1D marginal 68% MCIs for $\Omega_m h$ as functions of k_{\max} using galaxy clustering data from SDSS-4 LRG (red/shaded region), 2dF (blue/dashed line) and SDSS-2 main (green/solid line). *Top:* No nonlinear correction is used. *Middle:* Correction with the P model. *Bottom:* Correction with the Q model. For comparison we show also the corresponding 68% MCI from WMAP-3 (grey/dotted line).

For both SDSS-4 LRG and SDSS-2 main, nonlinear correction clearly leads to better agreement with 2dF and with WMAP-3 at $k_{\max} \gtrsim 0.1 h \text{ Mpc}^{-1}$. In the case of SDSS-2 main, although the correction is not sufficient to cause the 68% region to overlap with that from 2dF (using the same correction method), the two 95% regions are certainly consistent. Importantly, the level of disagreement between SDSS-2 main and 2dF after correction is no worse than the small internal inconsistency between the low and the high k_{\max} constraints on $\Omega_m h$ from SDSS-4 LRG already discussed in section 4.2. Thus if we should accept that the nonlinear models (1.1) and (1.2) offer

Table 2. 1D marginal 68% (95%) MCIs for $\Omega_m h$ and the nonlinear parameters P_{shot} and Q_{nl} from the three galaxy clustering data sets under consideration. We show results for $k_{\text{max}} \sim 0.2 h \text{ Mpc}^{-1}$ ($k_{\text{max}} \sim 0.18 h \text{ Mpc}^{-1}$ for 2dF), using (i) no nonlinear correction, (ii) correction with the P model, and (iii) correction with the Q model. The WMAP-3 preferred regions are also quoted here for comparison.

Data set	No correction	P model	Q model
$\Omega_m h$			
SDSS-4 LRG	0.234–0.252 (0.227–0.262)	0.163–0.184 (0.153–0.195)	0.169–0.191 (0.158–0.202)
2dF	0.167–0.204 (0.152–0.228)	0.134–0.173 (0.122–0.196)	0.134–0.178 (0.118–0.207)
SDSS-2 main	0.233–0.277 (0.213–0.300)	0.190–0.250 (0.167–0.279)	0.193–0.276 (0.167–0.316)
WMAP-3		0.159–0.195 (0.142–0.211)	
P_{shot} or Q_{nl}			
SDSS-4 LRG	–	3980–5170 (3380–5740)	22.7–25.5 (18.6–37.9)
2dF	–	452–1310 (< 1640)	7.0–19.2 (2.5–27.3)
SDSS-2 main	–	< 506 (< 831)	< 10.2 (< 19.5)

sufficient correction for SDSS-4 LRG, logically we must also consider them adequate for SDSS-2 main.

Lastly, we observe in figure 4 that the 2dF preferred values of $\Omega_m h$ tend in any case to be on the low side of SDSS-2 main, even at values of k_{max} well below those at which nonlinearity nominally sets in. This suggests that the residual inconsistency after nonlinear correction can rather be put down to a statistical aberration at small k values, than is indicative of a failure of either nonlinear model. Indeed, Sanchez and Cole [26] compared directly the power spectra of red galaxies (believed to be the main source of scale-dependent biasing) from 2dF and the main galaxy sample of SDSS data release 5, and found a similar discrepancy in the raw power spectrum data (see figure 7 of their paper). Our SDSS-2 main data set is but a subsample of SDSS data release 5; that it contains the same small fluctuation should be of no surprise.

5. Test 2: vanilla+massive neutrinos

It is well known that a subdominant component of massive neutrino HDM in the matter content slows down the growth of density perturbations on small length scales. In terms of the matter power spectrum, we expect a suppression of power of order $\Delta P_{\text{lin}}/P_{\text{lin}} \sim 8 \Omega_\nu/\Omega_m$ at $k \gg k_{\text{FS}}$, where k_{FS} is the neutrinos’ free-streaming wavenumber, and Ω_ν the neutrino energy density. Since this suppression effectively changes the shape of the matter power spectrum at large wavenumbers, some amount of degeneracy could conceivably exist between the neutrino energy density and the nonlinear correction parameters. In this section we investigate the possible existence of such a degeneracy, and if so, its effects on massive neutrino cosmology.

Table 3. 1D marginal 68% (95%) MCIs for $\Omega_m h$, f_ν , and the nonlinear parameters P_{shot} and Q_{nl} from SDSS-4 LRG, and the associated minimum χ^2 values. These are obtained using (i) no nonlinear correction, (ii) correction with the P model, and (iii) correction with the Q model. We quote here also the WMAP-3 preferred regions for comparison.

Model	$\Omega_m h$	f_ν	P_{shot} or Q_{nl}	χ_{min}^2
No correction	0.246–0.287 (0.232–0.314)	0.01–0.047 (< 0.065)	–	63.2
P model	0.168–0.216 (0.154–0.256)	< 0.057 (< 0.112)	4070–5270 (3430–5810)	19.7
Q model	0.171–0.226 (0.158–0.274)	< 0.061 (< 0.135)	23.6–36.9 (17.5–47.5)	20.6
WMAP-3	0.178–0.245 (0.151–0.270)	< 0.080 (< 0.127)	–	–

5.1. Set-up

We consider three parameter spaces:

- (i) $f_\nu, \Omega_m h, \Omega_b h^2, h, n_s, \ln(10^{10} \mathcal{A})$,
- (ii) $f_\nu, \Omega_m h, \Omega_b h^2, h, n_s, \ln(10^{10} \mathcal{A}), P_{\text{shot}}$, and
- (iii) $f_\nu, \Omega_m h, \Omega_b h^2, h, n_s, \ln(10^{10} \mathcal{A}), Q_{\text{nl}}$.

Here, the neutrino fraction $f_\nu \equiv \Omega_\nu / \Omega_m$ is defined as the ratio of the neutrino energy density Ω_ν to the total matter density Ω_m . The former is given by the well known expression

$$\Omega_\nu h^2 = \frac{\sum m_\nu}{93 \text{ eV}}, \quad (5.1)$$

where $\sum m_\nu$ denotes the sum of the neutrino masses. We assume 3.04 degenerate neutrino species, which should be a good approximation since neither CMB nor galaxy clustering measurements are at present sufficiently sensitive to $\sum m_\nu \lesssim 0.3 \text{ eV}$, where one might expect some small effects due to the neutrino mass hierarchy.

We fit these three cases to SDSS-4 LRG up to $k_{\text{max}} \sim 0.2 h \text{ Mpc}^{-1}$, using no nonlinear correction in case (i), and correction with the P and the Q model respectively for cases (ii) and (iii). As in the previous section, we impose WMAP-3 priors on the parameters h , n_s , and $\Omega_b h^2$ tabulated in table 1. Note that these priors differ from those used previously, since CMB constraints are model-dependent. We adopt a top-hat prior on f_ν , 0–0.5, while for Q_{nl} we use 0–100, in anticipation that more nonlinear correction may be required to offset the higher $\Omega_m h$ values usually inferred in cosmologies with massive neutrinos.

5.2. Results and discussions

Table 3 shows the 1D 68% and 95% MCIs for $\Omega_m h$, f_ν , and the nonlinear parameters P_{shot} and Q_{nl} for the three cases considered. We also give the minimum χ^2 values as a measure of the goodness-of-fit.

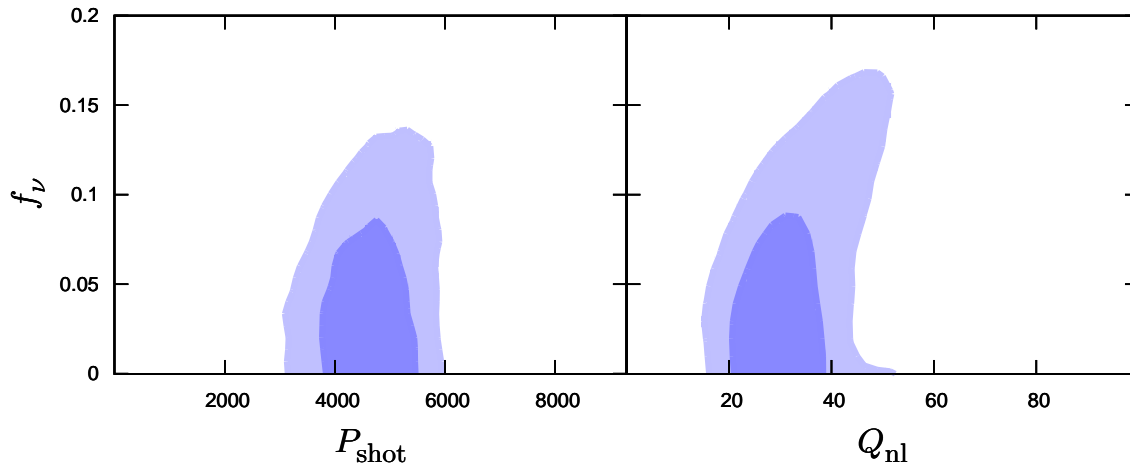


Figure 5. 2D marginal 68% and 95% MCIs for $\{f_\nu, P_{\text{shot}}\}$ and $\{f_\nu, Q_{\text{nl}}\}$ from SDSS-4 LRG, for cases (ii) and (iii) of section 5.1.

As in the case for vanilla cosmology, fitting the SDSS-4 LRG data without nonlinear correction leads to a very poor goodness-of-fit; the χ^2_{min} value is 63.2, for approximately $20 + 3 - 6 = 17$ degrees of freedom (20 data points of SDSS-4 LRG, 3 for the priors on n_s , h and $\Omega_b h^2$, and -6 for 6 free parameters). Adding nonlinear correction reduces χ^2_{min} by more than 40 units at the expense of only one extra parameter. Again, both nonlinear models offer very similar corrections to the power spectrum in terms of the inferred $\Omega_m h$ and f_ν values, although the P model appears to provide a slightly better fit to the data judging by its slightly smaller χ^2_{min} . Interestingly, despite the dramatic decrease in the minimum χ^2 between correction and no correction, the resulting shifts in the $\Omega_m h$ and f_ν estimates are deceptively small so that the 95% MCIs remain compatible before and after correction.

In the absence of nonlinear correction, the 95% upper limit on f_ν is about a factor of two too tight compared with the corrected case. This situation is reminiscent of the overly constraining bounds on $\sum m_\nu$ derived in some recent combined analyses of WMAP-3 and the flux power spectrum of the Lyman- α forest [50]. Too much power at large wavenumbers—either because of uncorrected nonlinearities in the galaxy power spectrum or an unusually large normalisation in the case of the Lyman- α forest—leads to the appearance of an overly flat matter power spectrum, which in turn prefers a smaller neutrino fraction and hence a smaller neutrino mass. The difference between the two corrected f_ν bounds is about 20%. The corresponding 95% limits on $\sum m_\nu$, < 1.76 eV for the P model and < 1.83 eV for the Q model, differ by even less. Thus cosmological neutrino mass determination is at present unaffected by our choice of nonlinear correction model.

Finally, we see in figure 5 that no strong degeneracy exists between the neutrino fraction f_ν and the nonlinear correction parameters P_{shot} and Q_{nl} . For small values of f_ν , the changes induced in the linear matter power spectrum by massive neutrino dark matter can be approximately mimicked by a redefinition of the apparent $\Omega_m h$

parameter [7],

$$(\Omega_m h)_{\text{apparent}} = (\Omega_m h)_{\text{true}} - 1.2 f_\nu, \quad (5.2)$$

assuming $h \sim 0.7$. Here, $(\Omega_m h)_{\text{apparent}}$ is the parameter that is actually constrained by power spectrum data, while $(\Omega_m h)_{\text{true}}$ denotes the true value of $\Omega_m h$. This expression also encapsulates the well known (approximate) degeneracy between $\Omega_m h$ and f_ν . Larger f_ν values induce more complicated changes in the power spectrum, and it is reassuring to see that these changes are not degenerate with nonlinear correction using either model.

6. The pathology of the Q model: vanilla+thermal axions

While both nonlinear models work very well for vanilla and for vanilla+massive neutrino cosmologies, and we may be tempted to conclude that they are for all purposes phenomenologically identical, we provide in this section a counter-example in which the incorrect functional form of the Q model can lead to some misleading results.

The case in point is a class of models containing a possible subdominant HDM component due to relic thermal axions with mass m_a . These models differ from those with massive neutrino HDM in that the temperature $T_a = [10.75/g_D^*(m_a)]^{1/3} T_\nu$ and hence the number density $n_a = [\zeta(3)/\pi^2] T_a^3$ of the axions are functions of m_a , since m_a determines when the particle species should decouple from the primordial plasma. Here, the function $g_D^*(m_a)$ denotes the effective number of thermal degrees of freedom at the time of decoupling, and must be calculated by carefully tracking the freeze-out process (e.g., [16]).

Thus, although qualitatively thermal axion HDM exhibits free-streaming features very similar to those of massive neutrinos, quantitatively the suppression of small scale power in the matter power spectrum has a nonlinear dependence on the axion mass. We show in this section how this nontrivial dependence can cause some problems for the Q model.

6.1. Set-up

We consider three parameter spaces:

- (i) $m_a, \Omega_m h, \Omega_b h^2, h, n_s, \ln(10^{10} A_s), b, Q_{\text{nl}}$, with a top-hat prior 0–100 on Q_{nl} ,
- (ii) $m_a, \Omega_m h, \Omega_b h^2, h, n_s, \ln(10^{10} A_s), b, Q_{\text{nl}}$, with a top-hat prior 0–200 on Q_{nl} , and
- (iii) $m_a, \Omega_m h, \Omega_b h^2, h, n_s, \ln(10^{10} A_s), b, P_{\text{shot}}$.

Cases (i) and (ii) both use the nonlinear model (1.1), and differ only in the priors imposed on the correction parameter Q_{nl} . Case (iii) uses the nonlinear model (1.2), with the usual prior on P_{shot} (see table 1). We fit each case to the combined data set WMAP-3+SDSS-4 LRG, using data up to $k_{\text{max}} \sim 0.2 h \text{ Mpc}^{-1}$ for the latter.

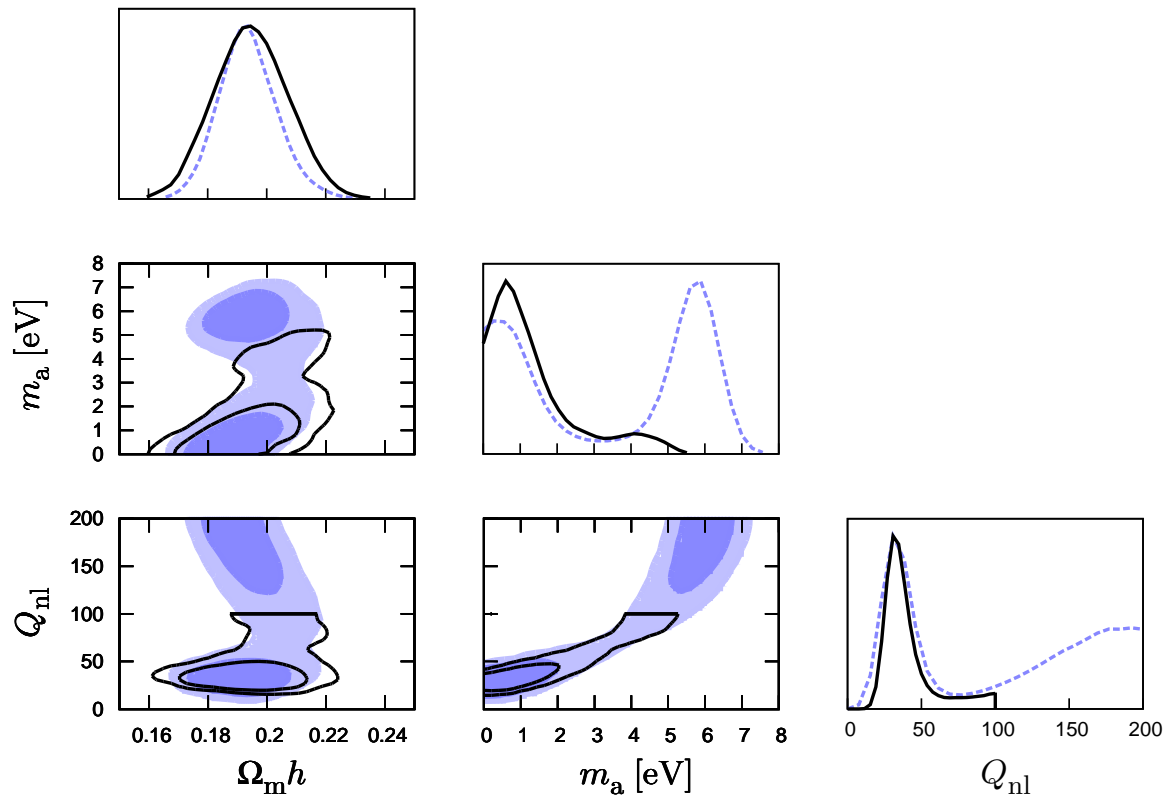


Figure 6. 2D marginal 68% and 95% MCIs for $\{\Omega_m h, m_a\}$, $\{\Omega_m h, Q_{\text{nl}}\}$, and $\{m_a, Q_{\text{nl}}\}$ from WMAP-3+SDSS-4 LRG. In the diagonal are the 1D marginal posteriors for the three named parameters. Black/solid lines correspond to case (i) of section 6.1 with a top-hat prior 0–100 on Q_{nl} , while the blue/shaded regions and blue/dashed lines denote case (ii) with Q_{nl} prior 0–200.

6.2. Results and discussions

Figure 6 shows the 2D marginal 68% and 95% MCIs for $\{\Omega_m h, m_a\}$, $\{\Omega_m h, Q_{\text{nl}}\}$, and $\{m_a, Q_{\text{nl}}\}$, as well as the 1D marginal posteriors for the the same three parameters for cases (i) and (ii).

Consider first the 1D marginal posteriors for Q_{nl} . We see in figure 6 that the posteriors in both cases (i) and (ii) remain finite all the way up to the upper limit of the prior imposed on Q_{nl} . This is also reflected in the relevant 2D contours, which are abruptly cut off at $Q_{\text{nl}} = 100$ and $Q_{\text{nl}} = 200$ respectively. Data alone does not constrain Q_{nl} in this class of cosmological models.

While this does not affect the $\Omega_m h$ estimates, the inference of the axion mass m_a depends crucially on how well we can constrain Q_{nl} because of a persisting degeneracy between the two parameters. Indeed, if we do not cut off Q_{nl} by hand at some sufficiently small value, a second peak begins to appear in the posterior at $\{m_a \sim 6 \text{ eV}, Q_{\text{nl}} \sim 200\}$, besides the one at $\{m_a \sim 0 \text{ eV}, Q_{\text{nl}} \sim 30\}$. From figure 7 we see that the power spectra for the two peaks after nonlinear correction are almost perfectly degenerate up to (and beyond) $k \sim 0.2 h \text{ Mpc}^{-1}$, even though the corresponding linear matter power spectra

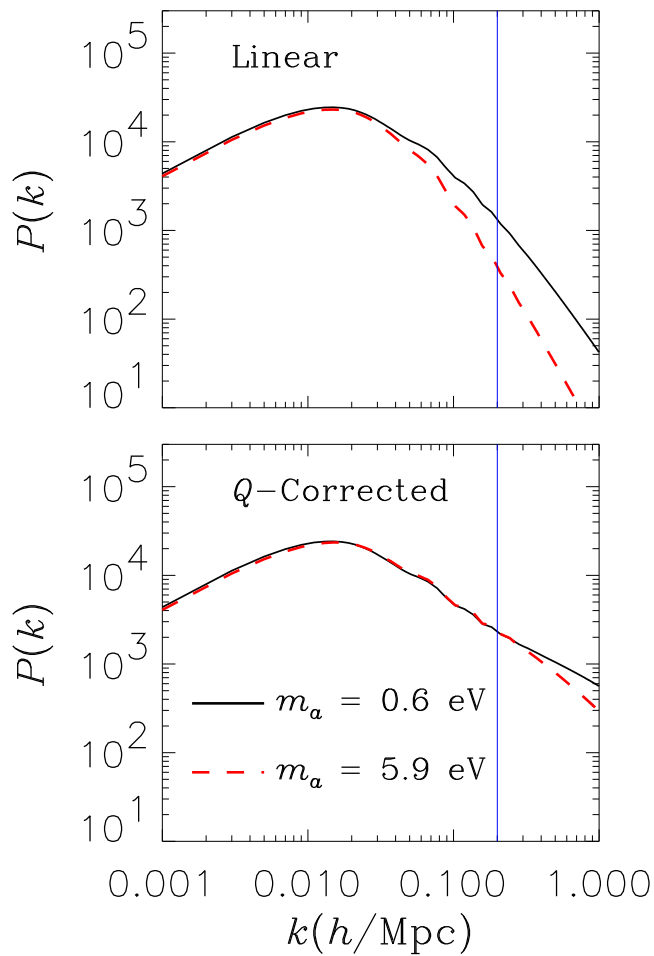


Figure 7. Matter power spectra for the two peak values of m_a . The black/solid lines are for $\{m_a = 0.6 \text{ eV}, Q_{\text{nl}} = 31\}$, and the red/dashed lines for $\{m_a = 5.9 \text{ eV}, Q_{\text{nl}} = 170\}$. The upper panel shows the linear matter power spectra, while the lower panel includes nonlinear correction with the Q model. The vertical line indicates the maximum value of k used in the analyses.

differ markedly already at $k \sim 0.04 h \text{ Mpc}^{-1}$.

We may be inclined to regard a 6 eV axion and, by implication, a large Q_{nl} value as unphysical because the former runs in conflict with constraints on m_a derived from stellar energy loss arguments and from telescope searches for axion radiative decays [51]. Furthermore, the m_a, Q_{nl} -degeneracy exists only in a limited k range: as shown in figure 7, the corrected power spectra for the two peaks begin to deviate at $k \gtrsim 0.3 h \text{ Mpc}^{-1}$. This suggests that the exact location of the high m_a peak in $\{m_a, Q_{\text{nl}}\}$ -space may in fact depend on our choice of k_{max} . Naturally we could have avoided this second peak simply by demanding consistency with other astrophysical constraints on m_a . However, in the absence of, e.g., galaxy formation simulations for this very class of cosmological models, we have *a priori* no reason to reject $Q_{\text{nl}} \sim 200$ or any other higher or lower value besides our own prejudices. Moreover, even if we manage to avoid the second peak with a finely tuned prior on Q_{nl} , the m_a, Q_{nl} -degeneracy means

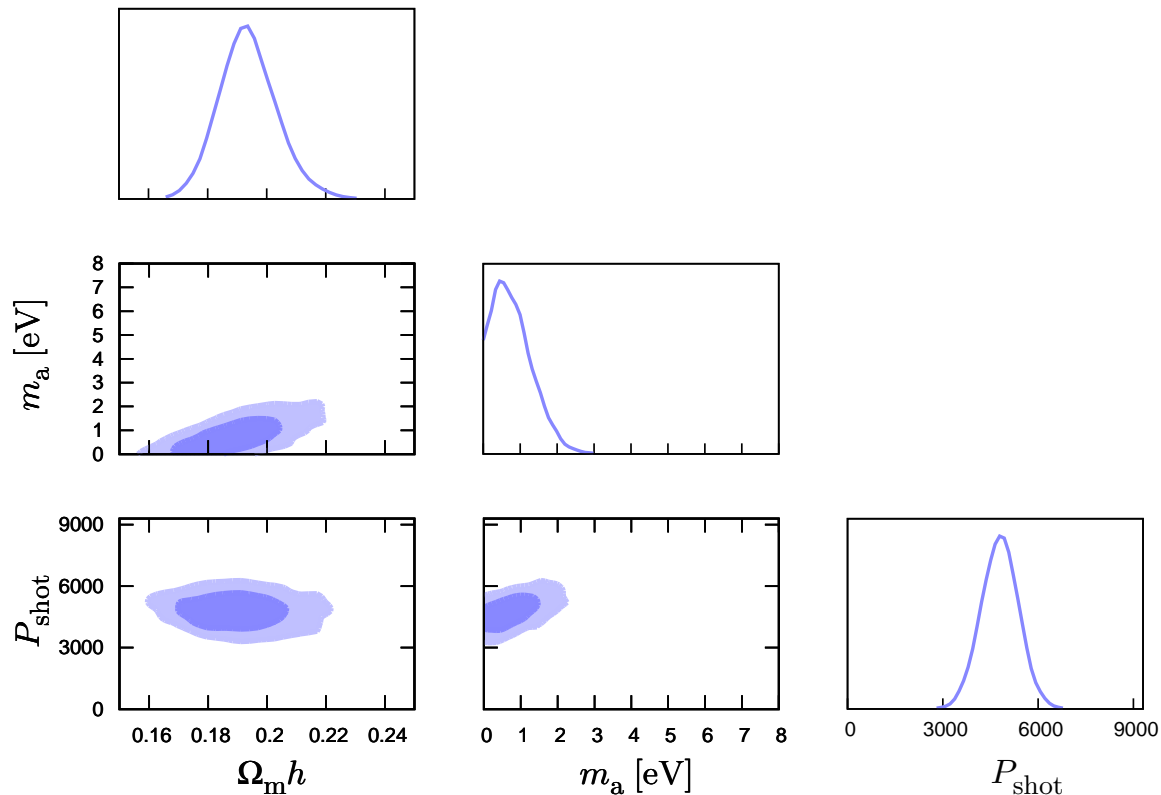


Figure 8. 2D marginal 68% and 95% MCIs for $\{\Omega_m h, m_a\}$, $\{\Omega_m h, P_{\text{shot}}\}$, and $\{m_a, P_{\text{shot}}\}$ from WMAP-3+SDSS-4 LRG for case (iii) of section 6.1. 1D marginal posteriors for the same three parameters are shown in the diagonal.

that the constraint thus obtained on m_a will still depend sensitively on exactly what we choose to be the upper limit of that prior.

This exercise also highlights the danger of analytic marginalisation [47], a technique sometimes used on nuisance parameters in COSMOMC to shorten the computation time. Here, analytic integration of the posterior in the direction of a nuisance parameter is made possible by taking the lower and upper limits of the parameter’s top-hat prior to $-\infty$ and ∞ respectively. Using this technique on the marginalisation of Q_{nl} , we find a unimodal 1D posterior for m_a whose 95% MCI of $4.95 \lesssim m_a/\text{eV} \lesssim 7.17$ favours unambiguously the high m_a region. Thus, analytic marginalisation can be very useful if the likelihood function itself sufficiently constrains the nuisance parameters. Otherwise, as we have seen here, the end results are potentially misleading.

Finally, we note that the P model does not suffer these problems. Figure 8 shows the 2D marginal 68% and 95% MCIs for $\{\Omega_m h, m_a\}$, $\{\Omega_m h, P_{\text{shot}}\}$, and $\{m_a, P_{\text{shot}}\}$, and the corresponding 1D marginal posteriors for case (iii). Here, although the correction parameter P_{shot} is slightly degenerate with the axion mass m_a , it is independently well constrained by data. Importantly, even if data fails to constrain P_{shot} , we have a simple and well defined way to choose our prior on P_{shot} . Thus we conclude that the P model is at present superior to the Q model for nonlinear correction in non-vanilla cosmologies.

7. Conclusions

In this paper we have explored two nonlinear correction and scale-dependent bias models—the Q model of reference [7] and the halo model-inspired P model—in some detail. We have confronted them with a range of galaxy clustering data and cosmologies to determine the strengths and weaknesses of the models.

In the context of standard Λ CDM cosmology, we find that both models perform equally well on present galaxy power spectrum data, in the sense that their corrective effects on the matter power spectrum are essentially identical. The case for nonlinear correction is very strong for the SDSS-4 LRG power spectrum. An indicative figure of merit is the minimum χ^2 : fitting data up to $k_{\text{max}} \sim 0.2 h \text{ Mpc}^{-1}$, we find that χ_{min}^2 changes from ~ 60 for 18 degrees of freedom without correction to ~ 20 for 17 degrees of freedom with correction, irrespective of the nonlinear model used. For 2dF and SDSS-2 main, however, the need for correction is marginal and subsists primarily because their respective $\Omega_m h$ estimates show better agreement with than without nonlinear correction. The preferred values of $\Omega_m h$ from SDSS-4 LRG, SDSS-2 main, and 2dF after correction, as well as from WMAP-3 can all be reconciled at 95% confidence, contrary to the case without correction.

Similar results are obtained for Λ CDM cosmologies extended with a subdominant component of massive neutrino hot dark matter. Data again show no strong preference for either nonlinear correction model, nor do we find any detrimental degeneracy between the neutrino fraction f_ν and either nonlinear correction parameter. Cosmological neutrino mass determination is at the time being unaffected by our choice of nonlinear correction model.

However, if the subdominant free-streaming dark matter is in the form of relic thermal axions, a nontrivial degeneracy between the axion mass m_a and the correction parameter Q_{nl} renders the Q model highly pathological, so that our inference of m_a depends sensitively on the prior we impose on Q_{nl} . In contrast, the P model, whose functional form is based on well motivated physics, does not suffer from this problem, and is arguably superior to the Q model. Note that we have used relic thermal axions here as an example. But our results may also be relevant for other light thermal relics whose temperature and hence abundance depend on the mass of the particle.

More precise data from future galaxy redshift surveys will eventually render these simplistic models inadequate to describe nonlinear evolution and scale-dependent biasing. For example, the damping of baryon acoustic oscillations due to nonlinear mode-coupling will need to be factored into the game at some stage [28, 43, 44]. The advent of wide- and deep-field weak gravitational lensing surveys in the next decade as an alternative probe of the large scale structure distribution will circumvent some of these nonlinearity issues. But galaxy redshift surveys will remain an important tool for the observation of baryon acoustic oscillations, and nonlinear evolution/scale-dependent bias modelling will continue to constitute an important aspect of the cosmological analysis machinery.

Acknowledgements

We thank Alexia Schulz and Robert E. Smith for useful comments on the manuscript. We acknowledge use of computing resources from the Danish Center for Scientific Computing (DCSC).

References

- [1] G. Hinshaw *et al.*, “Five-Year Wilkinson Microwave Anisotropy Probe (WMAP) Observations: Data Processing, Sky Maps, and Basic Results,” arXiv:0803.0732 [astro-ph].
- [2] M. R. Nolta *et al.*, “Five-Year Wilkinson Microwave Anisotropy Probe (WMAP) Observations: Angular Power Spectra,” arXiv:0803.0593 [astro-ph].
- [3] C. L. Reichardt *et al.*, “High resolution CMB power spectrum from the complete ACBAR data set,” arXiv:0801.1491 [astro-ph].
- [4] W. C. Jones *et al.*, “A Measurement of the Angular Power Spectrum of the CMB Temperature Anisotropy from the 2003 Flight of Boomerang,” *Astrophys. J.* **647** (2006) 823 [arXiv:astro-ph/0507494].
- [5] F. Piacentini *et al.*, “A Measurement of the polarization-temperature angular cross power spectrum of the Cosmic Microwave Background from the 2003 flight of BOOMERANG,” *Astrophys. J.* **647** (2006) 833 [arXiv:astro-ph/0507507].
- [6] T. E. Montroy *et al.*, “A Measurement of the CMB Spectrum from the 2003 Flight of BOOMERANG,” *Astrophys. J.* **647** (2006) 813 [arXiv:astro-ph/0507514].
- [7] S. Cole *et al.* [The 2dFGRS Collaboration], “The 2dF Galaxy Redshift Survey: Power-spectrum analysis of the final dataset and cosmological implications,” *Mon. Not. Roy. Astron. Soc.* **362** (2005) 505 [arXiv:astro-ph/0501174].
- [8] M. Tegmark *et al.*, “Cosmological Constraints from the SDSS Luminous Red Galaxies,” *Phys. Rev. D* **74** (2006) 123507 [arXiv:astro-ph/0608632].
- [9] W. J. Percival *et al.*, “The shape of the SDSS DR5 galaxy power spectrum,” *Astrophys. J.* **657** (2007) 645 [arXiv:astro-ph/0608636].
- [10] A. G. Riess *et al.* [Supernova Search Team Collaboration], “Observational Evidence from Supernovae for an Accelerating Universe and a Cosmological Constant,” *Astron. J.* **116** (1998) 1009 [arXiv:astro-ph/9805201].
- [11] S. Perlmutter *et al.* [Supernova Cosmology Project Collaboration], “Measurements of Omega and Lambda from 42 High-Redshift Supernovae,” *Astrophys. J.* **517** (1999) 565 [arXiv:astro-ph/9812133].
- [12] W. Hu, D. J. Eisenstein and M. Tegmark, “Weighing neutrinos with galaxy surveys,” *Phys. Rev. Lett.* **80** (1998) 5255 [arXiv:astro-ph/9712057].
- [13] S. Hannestad, “Primordial neutrinos,” *Ann. Rev. Nucl. Part. Sci.* **56** (2006) 137 [arXiv:hep-ph/0602058].
- [14] J. Lesgourgues and S. Pastor, “Massive neutrinos and cosmology,” *Phys. Rept.* **429** (2006) 307 [arXiv:astro-ph/0603494].
- [15] S. Hannestad and G. Raffelt, “Cosmological mass limits on neutrinos, axions, and other light particles,” *JCAP* **0404** (2004) 008 [arXiv:hep-ph/0312154].
- [16] S. Hannestad, A. Mirizzi and G. Raffelt, “New cosmological mass limit on thermal relic axions,” *JCAP* **0507** (2005) 002 [arXiv:hep-ph/0504059].
- [17] S. Hannestad, A. Mirizzi, G. G. Raffelt and Y. Y. Y. Wong, “Cosmological constraints on neutrino plus axion hot dark matter,” *JCAP* **0708** (2007) 015 [arXiv:0706.4198 [astro-ph]].
- [18] S. Hannestad, A. Mirizzi, G. G. Raffelt and Y. Y. Y. Wong, “Cosmological constraints on neutrino plus axion hot dark matter: Update after WMAP-5,” to appear in *JCAP* [arXiv:0803.1585 [astro-ph]].

- [19] A. Melchiorri, O. Mena and A. Slosar, “An improved cosmological bound on the thermal axion mass,” *Phys. Rev. D* **76** (2007) 041303 [arXiv:0705.2695 [astro-ph]].
- [20] M. Viel, J. Lesgourgues, M. G. Haehnelt, S. Matarrese and A. Riotto, “Constraining warm dark matter candidates including sterile neutrinos and light gravitinos with WMAP and the Lyman-alpha forest,” *Phys. Rev. D* **71** (2005) 063534 [arXiv:astro-ph/0501562].
- [21] L. Covi, J. Hamann, A. Melchiorri, A. Slosar and I. Sorbera, “Inflation and WMAP three year data: Features have a future!,” *Phys. Rev. D* **74** (2006) 083509 [arXiv:astro-ph/0606452].
- [22] J. Hamann, L. Covi, A. Melchiorri and A. Slosar, “New constraints on oscillations in the primordial spectrum of inflationary perturbations,” *Phys. Rev. D* **76** (2007) 023503 [arXiv:astro-ph/0701380].
- [23] A. J. Benson, S. Cole, C. S. Frenk, C. M. Baugh and C. G. Lacey, “The Nature of Galaxy Bias and Clustering,” *Mon. Not. Roy. Astron. Soc.* **311** (2000) 793 [arXiv:astro-ph/9903343].
- [24] M. Blanton, R. Cen, J. P. Ostriker, M. A. Strauss and M. Tegmark, “Time evolution of galaxy formation and bias in cosmological simulations,” *Astrophys. J.* **531** (2000) 1 [arXiv:astro-ph/9903165].
- [25] S. Cole, A. G. Sanchez and S. Wilkins, “The Galaxy Power Spectrum: 2dFGRS-SDSS tension?,” arXiv:astro-ph/0611178.
- [26] A. G. Sanchez and S. Cole, “The galaxy power spectrum: precision cosmology from large scale structure?,” *Mon. Not. Roy. Astron. Soc.* **385** (2008) 830 [arXiv:0708.1517 [astro-ph]].
- [27] P. McDonald, “Clustering of dark matter tracers: renormalizing the bias parameters,” *Phys. Rev. D* **74** (2006) 103512 [Erratum-ibid. *D* **74** (2006) 129901] [arXiv:astro-ph/0609413].
- [28] R. E. Smith, R. Scoccimarro and R. K. Sheth, “The Scale Dependence of Halo and Galaxy Bias: Effects in Real Space,” *Phys. Rev. D* **75** (2007) 063512 [arXiv:astro-ph/0609547].
- [29] U. Seljak, “Analytic model for galaxy and dark matter clustering,” *Mon. Not. Roy. Astron. Soc.* **318** (2000) 203 [arXiv:astro-ph/0001493].
- [30] J. A. Peacock and R. E. Smith, “Halo occupation numbers and galaxy bias,” *Mon. Not. Roy. Astron. Soc.* **318** (2000) 1144 [arXiv:astro-ph/0005010].
- [31] C. P. Ma and J. N. Fry, “Deriving the Nonlinear Cosmological Power Spectrum and Bispectrum from Analytic Dark Matter Halo Profiles and Mass Functions,” *Astrophys. J.* **543** (2000) 503, [arXiv:astro-ph/0003343].
- [32] A. Cooray and R. Sheth, “Halo models of large scale structure,” *Phys. Rept.* **372** (2002) 1 [arXiv:astro-ph/0206508].
- [33] A. E. Schulz and M. J. White, “Scale-dependent bias and the halo model,” *Astropart. Phys.* **25** (2006) 172 [arXiv:astro-ph/0510100].
- [34] J. Guzik, G. Bernstein and R. E. Smith, “Systematic effects in the sound horizon scale measurements,” *Mon. Not. Roy. Astron. Soc.* **375** (2007) 1329 [arXiv:astro-ph/0605594].
- [35] U. Seljak, “Redshift space bias and beta from the halo model,” *Mon. Not. Roy. Astron. Soc.* **325** (2001) 1359 [arXiv:astro-ph/0009016].
- [36] M. Tegmark *et al.* [SDSS Collaboration], “Cosmological parameters from SDSS and WMAP,” *Phys. Rev. D* **69** (2004) 103501 [arXiv:astro-ph/0310723].
- [37] G. Hinshaw *et al.*, “Three-year Wilkinson Microwave Anisotropy Probe (WMAP) observations: Temperature analysis,” *Astrophys. J. Suppl.* **170** (2007) 288 [arXiv:astro-ph/0603451].
- [38] L. Page *et al.*, “Three year Wilkinson Microwave Anisotropy Probe (WMAP) observations: Polarization analysis,” *Astrophys. J. Suppl.* **170** (2007) 335 [arXiv:astro-ph/0603450].
- [39] D. N. Spergel *et al.*, “Wilkinson Microwave Anisotropy Probe (WMAP) three year results: Implications for cosmology,” *Astrophys. J. Suppl.* **170** (2007) 377 [arXiv:astro-ph/0603449].
- [40] Legacy Archive for Microwave Background Data Analysis (LAMBDA), <http://lambda.gsfc.nasa.gov>
- [41] Y. B. Zeldovich, “Gravitational instability: An Approximate theory for large density perturbations,” *Astron. Astrophys.* **5** (1970) 84.
- [42] R. E. Smith *et al.* [The Virgo Consortium Collaboration], “Stable clustering, the halo model

- and nonlinear cosmological power spectra,” *Mon. Not. Roy. Astron. Soc.* **341** (2003) 1311 [arXiv:astro-ph/0207664].
- [43] M. Crocce and R. Scoccimarro, “Nonlinear Evolution of Baryon Acoustic Oscillations,” *Phys. Rev. D* **77** (2008) 023533 [arXiv:0704.2783 [astro-ph]].
- [44] R. E. Smith, R. Scoccimarro and R. K. Sheth, “‘Eppur Si Muove’: On The Motion of the Acoustic Peak in the Correlation Function,” *Phys. Rev. D* **77** (2008) 043525 [arXiv:astro-ph/0703620].
- [45] E. Huff, A. E. Schulz, M. J. White, D. J. Schlegel and M. S. Warren, “Simulations of baryon oscillations,” *Astropart. Phys.* **26** (2007) 351 [arXiv:astro-ph/0607061].
- [46] M. J. White, “The redshift space power spectrum in the halo model,” *Mon. Not. Roy. Astron. Soc.* **321** (2001) 1 [arXiv:astro-ph/0005085].
- [47] A. Lewis and S. Bridle, “Cosmological parameters from CMB and other data: a Monte-Carlo approach,” *Phys. Rev. D* **66** (2002) 103511 [arXiv:astro-ph/0205436].
- [48] A. Lewis, Homepage, <http://cosmologist.info>
- [49] J. Hamann, S. Hannestad, G. G. Raffelt and Y. Y. Y. Wong, “Observational bounds on the cosmic radiation density,” *JCAP* **0708** (2007) 021 [arXiv:0705.0440 [astro-ph]].
- [50] U. Seljak, A. Slosar and P. McDonald, “Cosmological parameters from combining the Lyman-alpha forest with CMB, galaxy clustering and SN constraints,” *JCAP* **0610** (2006) 014 [arXiv:astro-ph/0604335].
- [51] G. G. Raffelt, “Astrophysical axion bounds,” *Lect. Notes Phys.* **741** (2008) 51 [arXiv:hep-ph/0611350].